Microglial contribution to synaptic uptake in the prefrontal cortex in schizophrenia

Microglial contribution to synaptic uptake in the prefrontal cortex in schizophrenia

Authors

Makis Tzioras[1,2], Anna J. Stevenson[1,2], Delphine Boche[3*], Tara L. Spires-Jones[1,2*]

Affiliations

[1] UK Dementia Research Institute, The University of Edinburgh, UK

[2] Centre for Brain Discovery Sciences, The University of Edinburgh, UK

[3] Clinical Neurosciences, Clinical and Experimental Sciences Academic Unit, Faculty of Medicine, University of Southampton, UK

*** Equal contribution**

Correspondence to:
Professor Tara L. Spires-Jones
1 George Square, EH8 9JZ, Edinburgh, UK
Email: Tara.Spires-Jones@ed.ac.uk
Tel: 0131 6511895

Keywords: schizophrenia; pre-frontal cortex; microglia; synapse; gliosis; phagocytosis; psychiatric disorder; post-mortem; immunohistochemistry

The data that support the findings of this study are available from the corresponding author upon reasonable request.

Manuscript word count: 1,430

Number of Figures: 1
Number of Tables: 2
Number of Supplementary Figures: 2

Efficient synaptic communication is crucial to maintain healthy behavioural and cognitive processes. In neurodevelopmental diseases, like schizophrenia, affected individuals can exhibit behavioural symptoms like psychosis, hallucinations and alterations in decision-making. A reduction in cortical grey matter volume and enlarged ventricles in the brains of schizophrenia cases has been consistently reported [1,2]. This reduction in cortical volume is likely to be an outcome of neuronal and synaptic loss, which has also been reported in schizophrenia but the results have varied between brain area and synaptic markers examined [3–7]. A meta-analysis of the expression of synaptic markers in the disease has shown reduced levels of pre-synaptic markers in the frontal cortex which are heavily implicated in schizophrenia, but not in unaffected areas like the temporal and occipital lobes [8]. Synapses are crucial mediators of brain communication [9], and so, such synaptic alterations can have an impact on brain network connectivity, a process known to be affected in schizophrenia [10]. There are several factors during brain development that influence brain connectivity, with non-neuronal contributors playing an important role in synaptic formation and network maturation [11,12]. One of these non-neuronal contributors are microglia, the resident brain immune cells and primary phagocytes of the brain [12,13]. Gliosis is commonly observed during loss of brain homeostasis. Microglia have also been shown to facilitate neural network shaping in development by phagocytosing synapses using the complement system [14]. However, microglia can be aberrantly involved in synaptic elimination in non-physiological contexts, as observed in animal models of Alzheimer's disease [15]. Here, we performed a human post-mortem study to investigate the role of microglia in synaptic engulfment in schizophrenia. We examined microglial burden using Iba1 which labels the microglial cytoplasm and reflects microglial motility and homeostasis. Iba1 is considered as a pan-microglial marker and has been observed to be increased in a subset of neurodegenerative diseases [16]. Our other microglial marker, CD68, labels the lysosomal compartment of microglia [17].

We studied post-mortem brains from 10 control and 10 schizophrenia cases from the dorsolateral prefrontal cortex (DLPFC) which is affected in schizophrenia [1]. Cortical sections were stained with Iba1 and CD68 to label microglia (Figure 1A-D). We observed that there was no difference in either Iba1 ($p=0.315$) or CD68 ($p=0.794$) area coverage of the cortex (burden) between the schizophrenia and control cohorts (Figure 1E, F) (full statistical results found in Supplementary Table 1). Furthermore, there was no difference in the co-localisation between CD68 and Iba1 in controls and schizophrenia brains ($p=0.639$), suggesting the co-expression of the two markers per single cell is unchanged (Figure 1G).

Though no difference in microglial burdens between the two cohorts was observed, we aimed to assess whether microglia were involved in synaptic engulfment in schizophrenia. To do this, we quantified the amount of co-localisation between synapsin I and CD68 (% area), as a measure of engulfed synaptic material in the microglial phago-lysosomal compartment (Figure 1H-M). Firstly, in our cohort we did not find a significant difference in the cortical area occupied by synapsin I staining between the schizophrenia and control groups ($p=0.956$) (Figure 1N). Furthermore, we found no difference in synaptic engulfment by microglia between the schizophrenia and control cases ($p=0.413$) (Figure 1O). Additionally, when we normalised this co-localisation to their respective CD68 or Iba1 burdens, there was still no statistical difference between schizophrenia and control tissue ($p=0.167$ and $p=0.964$ respectively) (Figure 1P&Q). Of note, we have also shown microglia are capable of ingesting other pre-synaptic proteins like synaptophysin, as well as the post-synaptic protein PSD-95 (Supplementary Figures 1 and 2). Our data therefore suggest that at the time of death, microglia do not appear to be involved in aberrant synaptic internalisation in patients with schizophrenia.

In human post-mortem tissue from both patients with schizophrenia and age-matched controls, we found pre-synaptic proteins inside microglial cells in the frontal cortex of the brain, but no difference in the levels of synaptic internalisation between the two groups. A limitation of our post-mortem tissue is that it provides a snapshot of the disease many years after onset, which does not address the mechanism involved in synaptic internalisation by microglia. A greater sample size in an independent cohort will be useful to assess the reproducibility of these results and to stratify by confounding variables like sex and age. This would also allow us to assess whether confounding factors like depression, psychosis, systemic inflammation, and use of antipsychotic drugs affect these microglial and synaptic interactions. Furthermore, we have looked through all six cortical layers in a non-biased manner, but we cannot exclude layer specific differences in gliosis, synapse loss, or synaptic engulfment by microglia. However, this study is unique by the type of assessment performed on schizophrenia tissue is scarce.

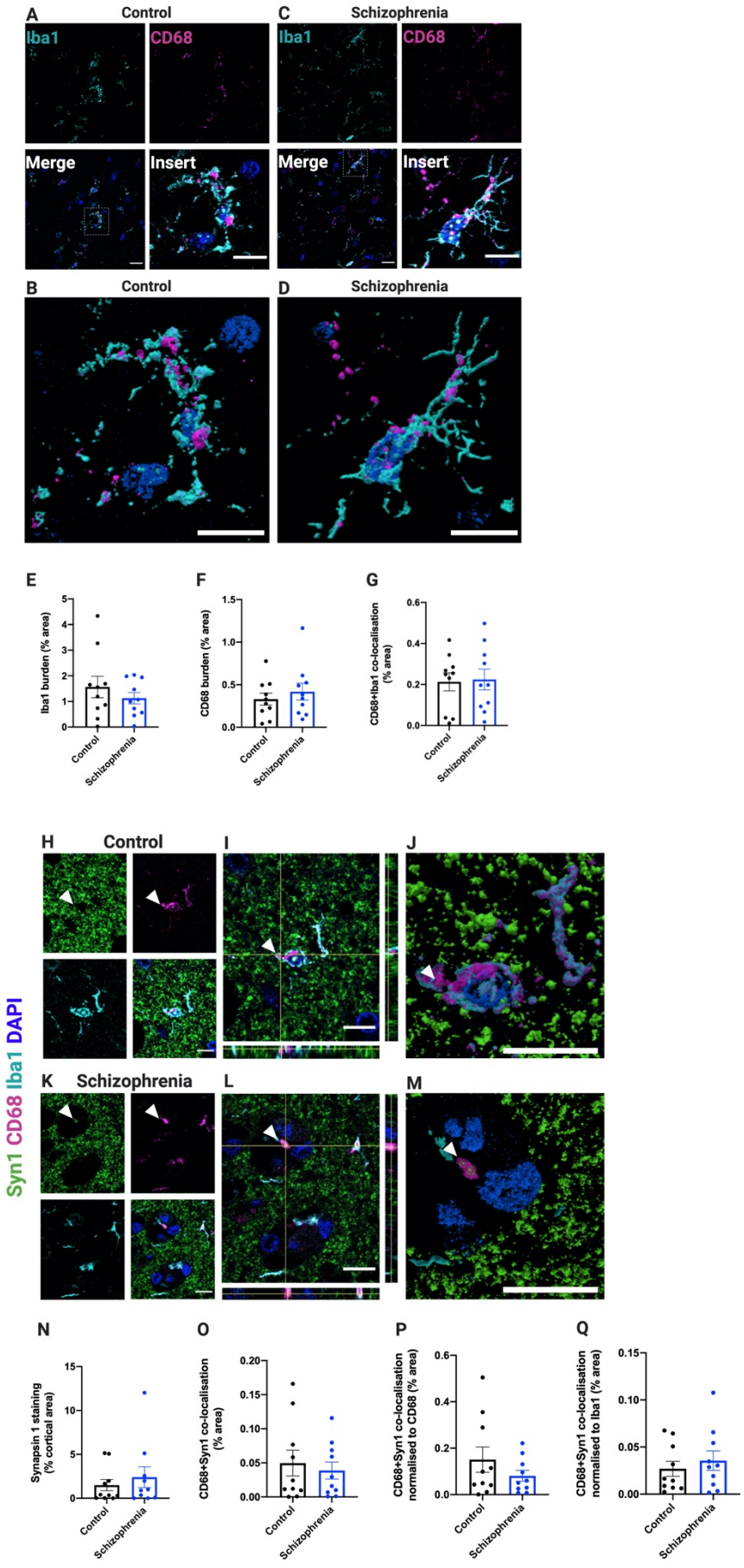
A
Control
Iba1
CD68
Merge
Insert
C
Schizophrenia
Iba1
CD68
Merge
Insert
B
Control
D
Schizophrenia
E
Iba1 burden (% area)
Control
Schizophrenia
F
CD68 burden (% area)
Control
Schizophrenia
G
CD68+Iba1 co-localisation (% area)
Control
Schizophrenia
H
Control
I
J
K
Schizophrenia
L
M
Syn1 CD68 Iba1 DAPI
N
Synapsin 1 staining (% cortical area)
Control
Schizophrenia
O
CD68+Syn1 co-localisation (% area)
Control
Schizophrenia
P
CD68+Syn1 co-localisation normalised to CD68 (% area)
Control
Schizophrenia
Q
CD68+Syn1 co-localisation normalised to Iba1 (% area)
Control
Schizophrenia

Figure 1. Microgliosis burdens unchanged in control and schizophrenia tissue. Representative confocal images of immunohistochemistry stained sections for the microglial markers Iba1 (cyan) and CD68 (magenta) in control (A and B) and schizophrenia (C and D) tissue. Nuclei are counterstained with DAPI. Scale bars in large images represent 20μm and 10μm in the expanded inserts (denoted by dotted white lines). The insert images of A and B are represented as 3D-reconstruction in B and D, respectively (scale bar, 10μm). 3-D reconstructions made on ParaView. Quantification of Iba1 burdens (% area), CD68 burdens (% area) and Iba1+CD68 co-expression (% area) are shown in panels E, F, and G, respectively. Representative confocal images of the pre-synaptic marker synapsin I (green) engulfed by CD68 (magenta) and Iba1 (cyan) in control (H-J) and schizophrenia tissue (K-M). H and K show individual panels of each stain and lastly the merged image, with white arrowheads pointing to sites of co-localisation between CD68 and synapsin I. I and L are expanded images of H and K, with orthogonal views indicating where CD68 and synapsin I co-localise inside Iba1 positive cells. J and M represent 3D reconstructions from H and K, generated on ParaView. Synapsin I burdens are shown in panel N. In O, the co-localisation index of CD68 and synapsin I is quantified for control and schizophrenia cases, where similar levels of synaptic engulfment by microglia are observed. By normalising each image to their respective CD68 burden or Iba1 burden there is still no statistical change in the engulfment of synapsin I by CD68 (P and Q, respectively). Each data point represents a mean average of 20 images taken per case, where n=10 per group. Linear mixed-effects model assessed statistical significance, considering $p \leq 0.05$ for significance. All scale bars in H-M represent 10μm.

With gliosis being reported in multiple brain disorders, we assessed microgliosis in schizophrenia. As described above, we found no differences in microglial burden between disease and control groups. This suggests that microglial activation is not a sustained event in chronic schizophrenia, and if any changes do occur in these cells it would instead likely involve functional alterations. Previous literature looking at CD68 expression in control and schizophrenia cases has also reported a similar outcome [18]. It is possible that if any changes in glial dynamics were to occur, they may be seen closer to disease onset, and that by the time the brains were donated ~35 years later, any changes would have subsided. This would be consistent with the observations published to visualise and quantify microglial activation *in vivo* with positron emission computed tomography (PET) using specific ligands of the translocator protein TSPO [19]. The PET studies have revealed that activated microglia are present in patients within the first 5 years of disease onset or during a psychotic state, whereas other PET studies in chronic schizophrenia have shown no difference in microglial activation between healthy controls and these patients. Nevertheless, TSPO signals are not a perfect read-out of microglia-mediated inflammation as they are influenced by age and are not microglia-specific [20,21].

Although developmental synaptic alterations, like synapse loss, have been characterised in individuals with schizophrenia [3,8], there are key unanswered questions that remain. For instance, it is not clear how the synapse elimination is mediated, the extent to which it drives behavioural symptoms, or whether it is the outcome of other disease-specific pathologies. Right now, a prominent mechanism for synaptic elimination in development is the use of the classical complement cascade (CCC), where it has been shown to sculpt neural circuits by tagging less electrically active synapses [14]. Recent research has now implicated complement as a signal for aberrant synapse elimination in disease [12,22]. Specifically, variants of C4 of the CCC are associated with a greater risk of developing schizophrenia [23], as well as poorer brain connectivity and schizophrenia-like behavioural deficits in mice [24].

Currently, a suggested mechanism by which complement-tagged synapses are cleared is by microglial recruitment for synaptic removal. In co-cultured neuron and microglia-like cells from human induced pluripotent stem cells from control and schizophrenia lines, increased levels of the excitatory post-synaptic protein PSD-95 was reported phagocytosed in the schizophrenia co-cultures [25]. Interestingly, this increased phagocytic activity was mainly driven by the presence of schizophrenia-derived microglia. Indeed, when schizophrenia neurons were co-cultured with microglia from control patients, the phagocytic index was reduced, indicating that in schizophrenia microglia have intrinsic differences in their phagocytic response. It is worth noting that induced stem cells are a good model for understanding human disease but represent a developmentally earlier phenotype, and not that of the age of the donor. Therefore, this supports a role for phagocytic microglia in early stages of the illness and may explain why we did not see any changes in phagocytic ability of microglia towards synapses in chronic schizophrenia, since we are not studying the developmental time-frame.

In conclusion, we report that microglia in human post-mortem tissue internalise pre-synaptic proteins physiologically, and that this does not appear to be altered in the chronic form of schizophrenia, in contrast with our observation in AD. Nevertheless, given the typically early onset of schizophrenia and that synapse loss is likely to have occurred years before brain collection, we cannot make assumptions on the role of microglia in synaptic clearance at the start of the disease. Looking forward, it would be interesting to study difference between young versus older cases in terms of synaptic uptake by microglia, and phenotype these changes in several brain areas to investigate any region-specific differences. Lastly, longitudinal PET

imaging of the pre-synaptic marker SV2A [26] and TSPO microglial marker would enable exploration of any microglia-synapse association during the course of the illnesses.

Methods

Human tissue

Ten cases with a confirmed diagnosis of schizophrenia (mean age 64.80 ± 20.37) and 10 non-neurological and non-neuropathological controls (mean age 64.40 ± 19.78) were obtained from the Corsellis Collection (Table 1). Dorsal prefrontal cortex (DPFC, or Brodmann area 46), an area showing neuroimaging abnormalities with reduction of the grey matter volume in chronic schizophrenia [1], was investigated for all cases. Cases with any other significant brain pathologies such as infarct, tumour, or traumatic brain injury were excluded from the study. Controls with no history of neurological or psychiatric disease or symptoms of cognitive impairment were matched to cases as possible. No difference in age at death and in post-mortem delay was detected between the 2 groups. To minimize the time in formalin, which has an effect on the quality of the immunostaining, the selection was performed on the availability of formalin-fixed paraffin embedded tissue, and thus on blocks processed at the time of the original post-mortem examination. Characteristics of the cohorts are provided in Table 1.

Table 1: Demographic, clinical and *post-mortem* characteristics of control and schizophrenia cases

Cases	**Ctrl (n=10)**	**Sz (n=10)**	**P value**
Sex	4F:6M	2F:8M	
Age at death (years, mean ± SD)	64.40 ± 19.78	64.80 ± 20.37	P = 0.94
Post-mortem delay (hours, mean ± SD)	61.90 ± 51.23	50.60 ± 24.52	P = 0.61
Age of onset (years, mean ± SD)	*NA*	36.50 ± 13.81	
Duration of illness (years, mean ± SD)	*NA*	35.13 ± 21.85	
Cause of death			
Cardiovascular disease	8	5	
infection/inflammation	1	3	
Trauma	1	1	
*Others**	0	1	

Ctrl, neurologically/cognitively normal controls; *Sz*, Schizophrenia cases; *F*, female, *M*, male; *SD*, standard deviation; *NA*, Not Applicable; *foreign body in respiratory tract

Immunohistochemistry

Paraffin-embedded tissue was cut at 7μm thickness on a microtome and mounted on Superfrost glass slides. The tissue was dewaxed in xylene, followed by rehydration in 100% EtOH, 90% EtOH, 70% EtOH, 50% EtOH, and finally water for 3 minutes each. Citric acid pH6 (VectorLabs, H-3300) was used for heat-mediated antigen retrieval by pressure cooking for 3 minutes at the steam setting. The slides were incubated for 5 minutes with autofluorescence eliminator reagent (Merck Millipore, 2160) to reduce background, followed by another 5 minutes incubation with Vector TrueView autofluorescence quenching kit (VectorLabs, SP-8400) to reduce red blood cell autofluorescence. Sections were blocked in 10% normal donkey serum (Sigma Aldrich, D9663-10ML) and 0.3% Triton X-100 (T8787-100ML) for 1 hour at room temperature. Microglia were stained with Iba1 (Abcam, ab5079, goat polyclonal, 1:500), and CD68 (DAKO, M0876, mouse monoclonal, 1:100), and pre-synaptic terminals with synapsin I (Sigma Aldrich, AB1543P, rabbit polyclonal, 1:750) or synaptophysin (R&D Systems, AF5555, goat polyclonal, 1:500) overnight at 4^{o}C in a humid chamber. For post-synaptic staining, PSD-95 was used to label excitatory post-synaptic densities (Synaptic Systems, 124 014, Guinea pig, 1:500), with the addition of salmon sperm DNA (Thermo Fisher Scientific, AM9680, diluted to 200μg/ml) in the blocking solution. All primary antibodies were diluted in the blocking solution described above. The following cross-adsorbed secondary antibodies were used: donkey anti-goat A647 (Thermo Fisher Scientific, A32849), donkey anti-mouse A594 (Thermo Fisher Scientific, A32744), and donkey anti-rabbit A488 (Thermo Fisher Scientific, A32790), donkey anti-Guinea pig A488 (Jackson Immunoresearch, 706-545-148). All secondary antibodies were diluted in phosphate buffer saline (PBS) (Thermo Fisher Scientific, 70011036). For tissue washes, 10X PBS was diluted in water to 1X concentration, with the addition of 0.3% Triton X-100 in washes prior to primary antibody incubation. Nuclei were counterstained with DAPI (1μg/ml) (D9542-10MG, Sigma-Aldrich).

Confocal microscopy and image analysis

Twenty images were taken randomly throughout all cortical layers of the grey matter for each case using a Leica TCS8 confocal microscope with a 63x oil immersion objective. Acquisition parameters were kept constant for all images and cases. Lif files were split into tiff files, and batch analysed on ImageJ (version 1.52p, Wayne Rasband, NIH, USA) using a custom co-localisation and thresholding macro. Images from different cases were also manually analysed to ensure the macro was accurately detecting positive signal and excluding background. For

synaptic internalisation by microglia we chose to analyse the colocalization of CD68 with Syn1, and also normalised to either CD68 or Iba1 burden. Data are expressed as protein burden (%) defined as the area fraction of each image labelled by the antibody. 3D reconstruction images were generated in ParaView 5.8.0. All experiments and analyses were blinded to the experimenter.

Ethics

Ethical approval was provided by BRAIN UK, a virtual brain bank which encompasses the archives of neuropathology departments in the UK and the Corsellis Collection, ethics reference 14/SC/0098. The study was registered under the Ethics and Research Governance (ERGO) of the Southampton University (Reference 19791).

Statistics

R Studio version 3.6.0 (2019-04-26) was used for statistical analysis [2]. Linear mixed-effects models were used to examine the effect of disease status on microglial burdens and CD68-Synapsin I co-localisation. This test was chosen because it allows all 20 images taken per case to be considered while accounting for non-independence, instead of a single mean value per case, allowing for a more powerful analysis on the results. QQ plots were generated in R Studio to check the residuals were normally distributed, which is an assumption of the mixed-effects model. To meet the assumptions of the test, all datasets were Tukey transformed prior to analysis (untransformed data presented in graphs). GraphPad Prism 8 was used for generating bar graphs with a mean value plotted per case, represented as a dot. We considered $p \leq 0.05$ as significant.

Acknowledgements

We would also like to thank our funders, specifically the UK Dementia Research Institute which receives funding from Alzheimer's Research UK, the Alzheimer's Society, and the Medical Research Council. We also would like to thank the Wellcome Trust for funding AJS and TLSJ. Tissue samples were obtained from The Corsellis Collection as part of the UK Brain Archive Information Network (BRAIN UK) which is funded by the Medical Research Council and Brain Tumour Research. Ethical approval was provided by BRAIN UK, a virtual brain bank which encompasses the archives of neuropathology departments in the UK and the Corsellis Collection, ethics reference 14/SC/0098. The study was registered under the Ethics and Research Governance (ERGO) of the Southampton University (Reference 19791). Authors contributed in the following ways: MT contributed in study design, performed experiments and imaging, statistical analysis, and manuscript preparation; AJS contributed in statistical analysis and manuscript editing; DB contributed by providing cut paraffin-embedded section, study design, and manuscript editing; TLSJ contributed with study design, statistical analysis, and manuscript editing. TLSJ is on the Scientific Advisory Board of Cognition Therapeutics and receives collaborative grant funding from 2 industry partners. None of these had any influence over the current paper. None of remaining authors declare any conflicting of interest. Figures created with BioRender.

References

1 Kikinis Z, Fallon JH, Niznikiewicz M, Nestor P, Davidson C, Bobrow L, *et al.* Gray matter volume reduction in rostral middle frontal gyrus in patients with chronic schizophrenia. *Schizophr Res* 2010;**123**:153–9.

2 Kahn RS, Sommer IE, Murray RM, Meyer-Lindenberg A, Weinberger DR, Cannon TD, *et al.* Schizophrenia. *Nat Rev Dis Primers* 2015;**1**:15067.

3 Feinberg I. Schizophrenia: caused by a fault in programmed synaptic elimination during adolescence? *J Psychiatr Res* 1982;**17**:319–34.

4 Faludi G, Mirnics K. Synaptic changes in the brain of subjects with schizophrenia. *Int J Dev Neurosci* 2011;**29**:305–9.

5 Onwordi EC, Halff EF, Whitehurst T, Mansur A, Cotel M-C, Wells L, *et al.* Synaptic density marker SV2A is reduced in schizophrenia patients and unaffected by antipsychotics in rats. *Nat Commun* 2020;**11**:246.

6 Browning MD, Dudek EM, Rapier JL, Leonard S, Freedman R. Significant reductions in synapsin but not synaptophysin specific activity in the brains of some schizophrenics. *Biol Psychiatry* 1993;**34**:529–35.

7 Funk AJ, Mielnik CA, Koene R, Newburn E, Ramsey AJ, Lipska BK, *et al.* Postsynaptic Density-95 Isoform Abnormalities in Schizophrenia. *Schizophr Bull* 2017;**43**:891–9.

8 Osimo EF, Beck K, Reis Marques T, Howes OD. Synaptic loss in schizophrenia: a meta-analysis and systematic review of synaptic protein and mRNA measures. *Mol Psychiatry* 2019;**24**:549–61.

9 Matsuzaki M, Ellis-Davies GC, Nemoto T, Miyashita Y, Iino M, Kasai H. Dendritic spine geometry is critical for AMPA receptor expression in hippocampal CA1 pyramidal neurons. *Nat Neurosci* 2001;**4**:1086–92.

10 Klauser P, Baker ST, Cropley VL, Bousman C, Fornito A, Cocchi L, *et al.* White matter disruptions in schizophrenia are spatially widespread and topologically converge on brain network hubs. *Schizophr Bull* 2017;**43**:425–35.

11 Eroglu C, Barres BA. Regulation of synaptic connectivity by glia. *Nature* 2010;**468**:223–31.

12 Henstridge CM, Tzioras M, Paolicelli RC. Glial contribution to excitatory and inhibitory synapse loss in neurodegeneration. *Front Cell Neurosci* 2019;**13**:63.

13 Sierra A, Abiega O, Shahraz A, Neumann H. Janus-faced microglia: beneficial and detrimental consequences of microglial phagocytosis. *Front Cell Neurosci* 2013;**7**:6.

14 Schafer DP, Lehrman EK, Kautzman AG, Koyama R, Mardinly AR, Yamasaki R, *et al.* Microglia sculpt postnatal neural circuits in an activity and complement-dependent manner. *Neuron* 2012;**74**:691–705.

15 Hong S, Beja-Glasser VF, Nfonoyim BM, Frouin A, Li S, Ramakrishnan S, *et al.* Complement and microglia mediate early synapse loss in Alzheimer mouse models. *Science* 2016;**352**:712–6.

16 Boche D, Perry VH, Nicoll JAR. Review: activation patterns of microglia and their identification in the human brain. *Neuropathol Appl Neurobiol* 2013;**39**:3–18.

17 Franco-Bocanegra DK, McAuley C, Nicoll JAR, Boche D. Molecular mechanisms of microglial motility: changes in ageing and alzheimer's disease. *Cells* 2019;**8**. doi:10.3390/cells8060639

18 Arnold SE, Trojanowski JQ, Gur RE, Blackwell P, Han LY, Choi C. Absence of neurodegeneration and neural injury in the cerebral cortex in a sample of elderly patients with schizophrenia. *Arch Gen Psychiatry* 1998;**55**:225–32.

19 De Picker LJ, Morrens M, Chance SA, Boche D. Microglia and Brain Plasticity in Acute Psychosis and Schizophrenia Illness Course: A Meta-Review. *Front Psychiatry* 2017;**8**:238.

20 De Picker L, Ottoy J, Verhaeghe J, Deleye S, Wyffels L, Fransen E, *et al.* State-associated changes in longitudinal [18F]-PBR111 TSPO PET imaging of psychosis patients: Evidence for the accelerated ageing hypothesis? *Brain Behav Immun* 2019;**77**:46–54.

21 Notter T, Schalbetter SM, Clifton NE, Mattei D, Richetto J, Thomas K, *et al.* Neuronal activity increases translocator protein (TSPO) levels. *Mol Psychiatry* Published Online First: 12 May 2020. doi:10.1038/s41380-020-0745-1

22 Carpanini SM, Torvell M, Morgan BP. Therapeutic inhibition of the complement system in diseases of the central nervous system. *Front Immunol* 2019;**10**:362.

23 Sekar A, Bialas AR, de Rivera H, Davis A, Hammond TR, Kamitaki N, *et al.* Schizophrenia risk from complex variation of complement component 4. *Nature* 2016;**530**:177–83.

24 Comer AL, Jinadasa T, Sriram B, Phadke RA, Kretsge LN, Nguyen TPH, *et al.* Increased expression of schizophrenia-associated gene C4 leads to hypoconnectivity of prefrontal cortex and reduced social interaction. *PLoS Biol* 2020;**18**:e3000604.

25 Sellgren CM, Gracias J, Watmuff B, Biag JD, Thanos JM, Whittredge PB, *et al.* Increased synapse elimination by microglia in schizophrenia patient-derived models of synaptic pruning. *Nat Neurosci* 2019;**22**:374–85.

26 Colom-Cadena M, Spires-Jones T, Zetterberg H, Blennow K, Caggiano A, DeKosky ST, *et al.* The clinical promise of biomarkers of synapse damage or loss in Alzheimer's disease. *Alzheimers Res Ther* 2020;**12**:21.

List of supplementary figure legends

Supplementary Table 1: Linear mixed-effects model outcomes from R Studio.

Measurement	Effect size	Standard Error	p-value
Iba1 burden (% area)	-0.1637	0.1580	0.315
CD68 burden (% area)	0.0165	0.06215	0.794
Synapsin 1 burden (% area)	0.01049	0.1862	0.956
CD68+Iba1 colocalisation (% area)	-0.0378	0.0792	0.639
CD68+Syn1 colocalisation (% area)	-0.0772	0.0917	0.413
CD68+Syn1 colocalisation /CD68 (% area)	-0.1414	0.0980	0.167
CD68+Syn1 colocalisation /Iba1 (% area)	-0.0044	0.0958	0.964

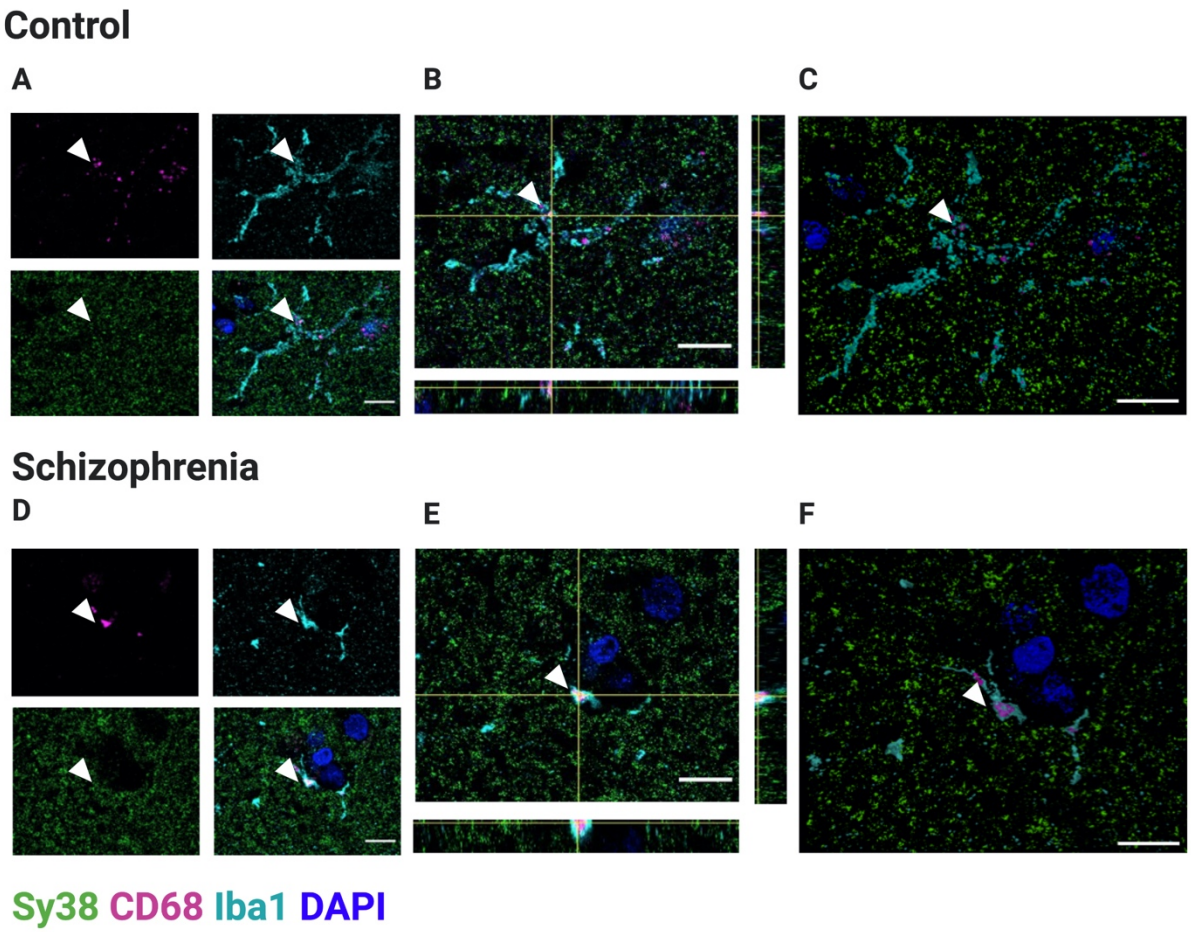

Supplementary Figure 1. Microglia can engulf synaptophysin in control and schizophrenia human post-mortem tissue. Representative confocal images of the pre-synaptic marker synaptophysin, Sy38, (green), CD68 (magenta) and Iba1 (cyan) in control (A-C) and schizophrenia tissue (D-F). Nuclei are counterstained with DAPI. A and D show individual panels of each stain and lastly the merged image, with white arrowheads pointing to sites of co-localisation between CD68 and synaptophysin. B and E are expanded images of A and D, with orthogonal views indicating where CD68 and synaptophysin co-localise. C and F represent 3D reconstructions from A and D, generated on ParaView. All scale bars represent 10µm.

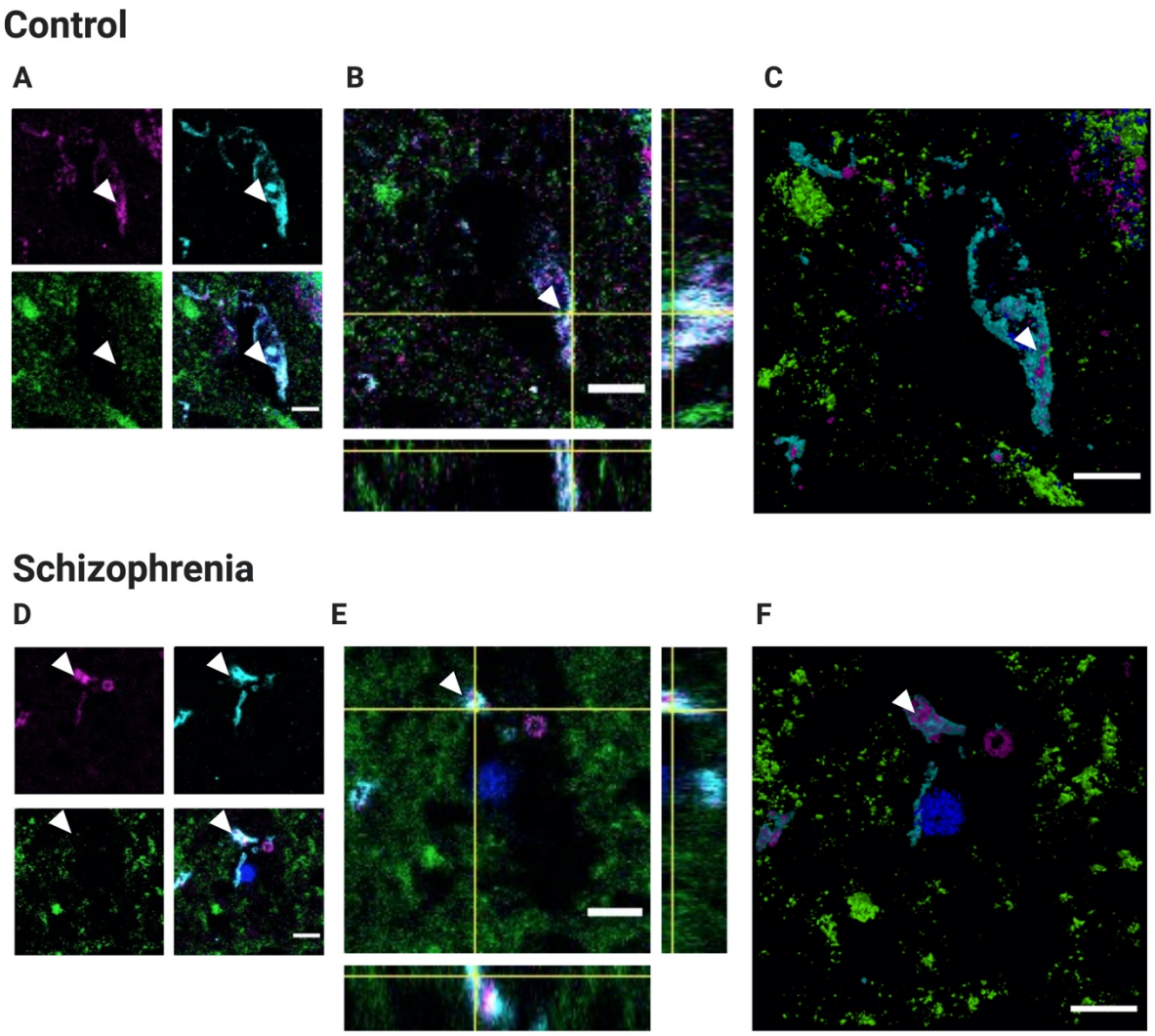

Supplementary Figure 2. Microglia can engulf PSD-95 in control and schizophrenia human post-mortem tissue. Representative confocal images of the pre-synaptic marker PSD-95 (green), CD68 (magenta) and Iba1 (cyan) in control (A-C) and schizophrenia tissue (D-F). Nuclei are counterstained with DAPI. A and D show individual panels of each stain and lastly the merged image, with white arrowheads pointing to sites of co-localisation between CD68 and PSD-95. B and E are expanded images of A and D, with orthogonal views indicating where CD68 and PSD-95 co-localise. C and F represent 3D reconstructions from A and D, generated on ParaView. All scale bars represent 5µm.